

A&A manuscript no.
(will be inserted by hand later)

Your thesaurus codes are:
06 (03.20.8; 03.13.5; 11.11.1;)

Interpreting the kinematics of the extended gas in distant radio galaxies from 8-10m telescope spectra.

M. Villar-Martín,¹ A. Alonso-Herrero,¹ S. di Serego Alighieri² and J. Vernet³

¹ Dept. of Natural Sciences, Univ. of Hertfordshire, College Lane, Hatfield, Herts AL10 9AB, UK

² Osservatorio Astrofisico di Arcetri, Largo E. Fermi 5, I-50125, Firenze, Italy

³ European Southern Observatory, Karl Schwarzschild Str. 2, D-85748 Garching, Germany

Abstract. The nature of the extreme kinematics in the extended gas of distant radio galaxies ($z > 0.7$) is still an open question. With the advent of the 8-10 m telescope generation and the development of NIR arrays we are in the position for the first time to develop a more detailed study by using lines other than Ly α and [OII] $\lambda 3727$ depending on redshift. In this paper we review the main sources of uncertainty in the interpretation of the emission line kinematics: the presence of several kinematic components, Ly α absorption by neutral gas/dust and the contribution of scattered light to some of the lines. As an example, several kinematic components can produce apparent, false rotation curves. We propose methods to solve these uncertainties.

We propose to extend the methods applied to low redshift radio galaxies to investigate the nature of the kinematics in distant radio galaxies: by means of the spectral decomposition of the strong optical emission lines (redshifted into the NIR) we can isolate the different kinematic components and study the *emission line ratios* for the individual components. If shocks are responsible for the extreme kinematics, we should be able to isolate a kinematic component (the shocked gas) with large FWHM ($\geq 900 \text{ km s}^{-1}$), low ionization level [OIII] $\lambda 5007/\text{H}\beta \sim 2.4$ and weak HeII $\lambda 4686/\text{H}\beta \leq 0.07$, together with a narrow component ($\leq \text{few hundred km s}^{-1}$) with higher ionization level and strong HeII emission (HeII/H $\beta \sim 0.5$)

Key words: Techniques: spectroscopic – Methods: observational – Galaxies, kinematics and dynamics

1. Introduction

High redshift radio galaxies ($z \geq 0.7$, HzRG) show optical regions of ionized gas that extend across tens (sometimes hundreds) of kiloparsecs. These structures are aligned with the radio axis (McCarthy et al. 1987, Chambers et al. 1987) and show very irregular and clumpy morphologies. The kinematics is extreme compared to the low redshift counterparts. Line widths (Ly α or [OII] $\lambda 3727$) as broad as $\text{FWHM} \geq 1000 \text{ km s}^{-1}$ are often measured (McCarthy et al. 1996, Villar-Martín, Binette & Fosbury 1999, Baum & McCarthy 2000) versus $\sim 300\text{--}400 \text{ km s}^{-1}$ commonly observed at low redshift (*e.g.* Tadhunter et al. 1989). Velocity dispersions range from several hundreds up to 1600 km s^{-1} and there are velocity shifts between different lines of up to $\sim 1000 \text{ km s}^{-1}$ (Röttgering et al. 1997). Baum & McCarthy (2000) showed that the transition from predominantly quiescent systems to those with extreme motions occurs near $z \sim 0.6$.

While at low redshift the kinematics of the extended gas in radio galaxies is generally explained in terms of gravitational motions, the mechanism responsible for the extreme motions at higher redshifts is not well understood. The apparent connection between the size of the radio source and the emission line kinematics observed at $z \geq 2$ (van Ojik et al. 1997) suggests interactions between the radio and optical structures that perturb the kinematics. This is supported by the discovery in some HzRG of haloes of ionized gas extending *beyond* the radio structures that emit *narrow* Ly α ($\sim 250 \text{ km s}^{-1}$) compared to the inner regions ($\sim 1200 \text{ km s}^{-1}$) (van Ojik et al. 1996).

Baum & McCarthy (2000) studied a much larger sample covering a wider range in redshift. They find *no* (or very weak) correlation between the emission line kinematics and the *ratio* of the radio to nebular size. The authors support a gravitational origin for the kinematics of HzRG. Bipolar outflows (possible consequence of a circumnuclear starburst) have also been proposed by some authors (*e.g.* Chambers 1998, Taniguchi & Shioya 2000).

Understanding the nature of the kinematics in HzRG will help to answer some open questions related to these galaxies:

- What is the nature of the alignment effect? Scattered light from the hidden AGN is an important contributor (*e.g.* Cimatti et al. 1997, 1998, Fosbury et al. 1999). However, the likely influence of radio jet/gas interactions is still not understood.
- The ionization processes in the extended gas of HzRG is clearly related to the nuclear activity, but what is the main mechanism: jet driven shocks or AGN illumination?
- How does the radio source interact with its environment and how does it influence the subsequent evolution of the system?
- Are very distant radio galaxies ($z \geq 2$) in proto clusters?

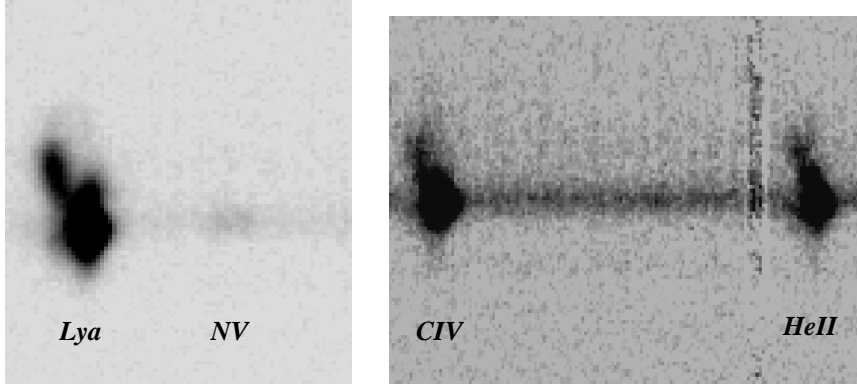


Fig. 1. KeckII+LRISp spectra of the HzRG B3 0731+438 ($z = 2.42$). The new generation of 8-10 m telescopes allows for the first time the detection of emission lines other than Ly α in the extended gas of very distant radio galaxies ($z \geq 2$) with high S/N.

To date, the kinematic studies of the gas in HzRG have been done in the optical. The main limitation has been the need for a large collecting area to detect the emission lines with high signal/noise ratio (S/N) in the extended gas. With 3-4m telescopes, only [OII] $\lambda 3727$ ($z < 1.2$) or Ly α ($z \geq 2$) could be used. At ($z \geq 2$) the uncertainties are important, since Ly α is highly sensitive to dust/neutral gas absorption. The strong optical (rest frame) emission lines ([OIII] $\lambda 5007, 4959$, [OII] $\lambda 3727$) are more reliable. However, they are redshifted into the NIR and the need for a large collecting area has constrained the NIR spectroscopic studies of HzRG (and quasars) to the spatially integrated properties (*e.g.* Jackson & Rawlings 1997, McIntosh et al. 1999, Larkin et al. 2000)

This is the epoch of the 8-10 meter telescope generation. We are in the position for the first time to study the kinematics of the extended gas in HzRG:

- using UV rest frame lines (redshifted into the optical) other than Ly α such as HeII, CIV or CIII] (see Fig. 1).
- using the optical rest frame lines such us [OIII] $\lambda 5007, 4949$, H α , etc (redshifted into the NIR). The development of NIR arrays (and large collecting areas) makes this study possible for the first time.

In spite of the opportunities opened by the new technological facilities, the study of the kinematic properties of HzRG is still complex. The goal of this paper is to assess the main sources of uncertainty and provide solutions to solve them.

2. The data

We present for illustrative purposes spectra of several high redshift radio galaxies ($z \sim 2.5$) obtained with the Low Resolution Imaging Spectrometer (LRISp, Oke et al. 1995) at the

Keck II telescope. Detailed description of the observing runs and data reduction will be presented in Vernet et al. (2001, in prep.).

3. Uncertainties on interpreting the kinematic properties of the extended gas in HzRG

The strongest lines in the optical (observed) spectra of HzRG are Ly α , CIV λ 1550, HeII λ 1640 and CIII λ 1909, while [OII] λ 3727, [OIII] $\lambda\lambda$ 5007,4959, H α dominate in the NIR. There are some physical effects that might make the interpretation of the line profiles and velocity shifts uncertain.

- Presence of multiple kinematic components
- Broad scattered lines
- Resonant scattering of Ly α and (maybe) CIV photons

3.1. Multiple kinematic components

We mentioned in §1 that the interaction between the radio jet and the ambient gas could be responsible for the extreme motions in HzRG. Other authors favour a gravitational origin for the kinematics of the gas. One interpretation or another has important consequences: if the velocity fields reflect the gravitational potential, the derived dynamical mass turns out to be correlated with redshift and/or radio power (Baum & McCarthy 2000). As the authors pointed out, this result is not valid if shocks are responsible for the kinematics.

Villar-Martín et al. (1999) carried out a detailed spectroscopic study of the intermediate redshift radio galaxy PKS2250-51 ($z = 0.31$) where a strong interaction between the radio and optical structures occurs. The authors resolved two main kinematic components, spatially extended and detected in all optical (rest frame) emission lines. One of the components is narrow (~ 150 -200 km s $^{-1}$), the line ratios are consistent with photoionization and it extends beyond the radio structures. The other component is broad (FWHM as large as 900 km s $^{-1}$ at some spatial positions), the line ratios are consistent with shock ionization and it is emitted inside the radio structures. The properties of the narrow component suggest that it is emitted by ambient photoionized gas that has not been perturbed, while the properties of the broad component are consistent with shocked gas.

A similar spectroscopic study could prove or disprove shocks as responsible for the kinematics in HzRG. The studies done so far have been based on the emission line kinematics along the radio axis and they have not provided a definitive answer. We propose that the joint study of the line kinematics (with spectral decomposition of the line profiles) and the line ratios may give the answer. If shocks perturb the kinematics

in HzRG, then we should expect similar components and with similar flux ratios as those observed in PKS2250-41. With 2D spectrographs it will be possible to extend the kinematic studies to regions far from the radio axis, where the interactions are expected to be non existent. The detection of broad lines far from the radio axis would confirm that jet/cloud interactions are not responsible for the extreme motions.

The spectral resolution we use is crucial to be able to isolate different kinematic components in the extended gas. A velocity resolution of $\sim 250 \text{ km s}^{-1}$ ($R = \lambda/\Delta\lambda \sim 1200$) would be ideal since it will allow an accurate decomposition of the emission line profiles. The instrumental profile (IP) is in this case well matched with the expected FWHM of the non perturbed gas (so that we avoid unnecessary instrumental broadening), such as the diffuse haloes extending beyond the radio structures. The study of such haloes can be very useful, since they show the gas properties before any perturbation. With the new 1024×1024 NIR arrays it should be possible to cover the interesting spectral range ($\text{HeII}\lambda 4686$ to $[\text{OIII}]\lambda 5007$) for a good number of objects.

3.1.1. Apparent rotation curves

The presence of several kinematic components can lead us to derive false rotation curves.

Fig. 2 shows two examples of HzRG where the emission lines show a resemblance with rotation curves (see also Fig. 1 and Fig. 2 in Villar-Martín, Binette & Fosbury 1999). This could be an exciting evidence for merger events (*e.g.* Hernquist 1993). However, the apparent rotation is an artifact, consequence of the presence of at least two kinematic components. To illustrate this, we have used the spectrum of the radio galaxy B3 0731+438 (Fig. 1). We have extracted 1-D spectra from those spatial pixels where the abrupt jump in the apparent rotation curve occurs. Fig. 3 shows the $\text{Ly}\alpha$ spectral profile at each pixel. The profile changes dramatically due to the presence of at least two kinematic components that contribute with different relative intensity at different pixels. Fig. 1 shows clearly the two main components. The fact that they are apparent also in HeII proves that it is not an effect of resonant scattering of $\text{Ly}\alpha$ and CIV. This makes the $\text{Ly}\alpha$ velocity centroid change in space, giving the appearance of a rotation curve. If we isolate the two components at every spatial position the rotation curve disappears (see Fig. 4).¹

¹ Misleading velocity curves can also be a result of instrumental effects. If the seeing disc is noticeably smaller than the slit width and our object is clumpy (which is the case of HzRG) the clumps occupy different spatial positions in the direction perpendicular to the slit. The centroid of the emission lines will be shifted in the spectral direction. Another negative effect is that the sky or arc lines may not represent the true instrumental profile and therefore we need to derive it from the seeing value or, better, from a point source along the slit.

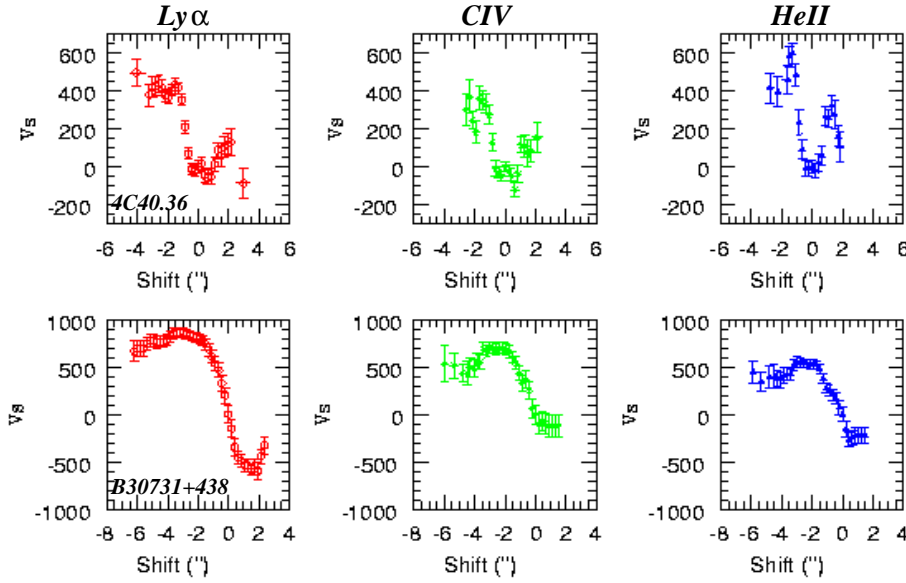


Fig. 2. Velocity curves of Ly α , CIV and HeII emission lines in 4C40.36 ($z=2.27$) (top panels) and B3 0731+438 ($z=2.43$) (bottom panels). The spatial zero has been defined at the position of the centroid of continuum emission in both cases. These velocity curves suggest rotation of the ionized gas.

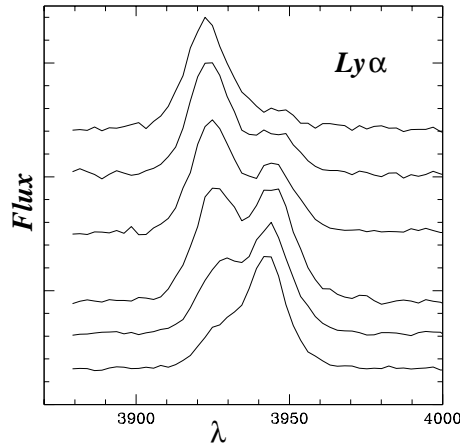


Fig. 3. Spatial variation of the spectral profile of Ly α in B3 0731+438. Each curve is the Ly α spectral profile (redshifted) at a given spatial position (pixel). Two kinematic components are present whose relative contributions change from pixel to pixel.

3.2. Broad scattered lines

Many HzRG are highly polarized in the optical due to the scattering of nuclear emission (both continuum and emission lines from the broad line region) by (probably) dust in the extended gas (e.g. Cimatti et al. 1997, 1998, Fosbury et al. 1999). The radiation from the extended gas is therefore a mixture of direct and scattered light. Can the scattered broad lines affect our conclusions on the kinematic studies if neglected?

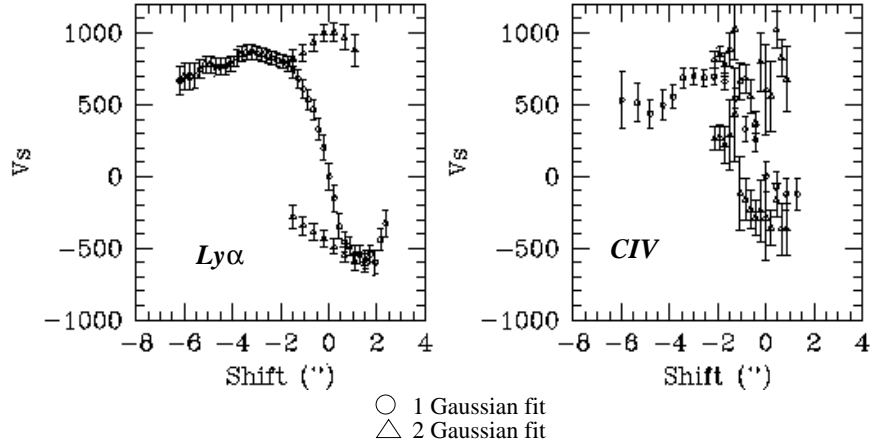


Fig. 4. Comparison between the results obtained by fitting 1 and 2 Gaussians to the spectral profile of the lines. The individual kinematic components are shown as open triangles and the result of fitting a single Gaussian is shown as open circles. The gradient in the velocity curve is due to the change on the contribution of one component relative to the other. The "apparent" rotation curve is an artifact consequence of the blend of both components in some pixels.

As an example we present the spectrum of TXS0211-122 ($z = 2.34$), one of the most highly polarized ($P \sim 20\%$ longward Ly α) radio galaxies at high redshift. We have analysed the profile of CIV, which is efficiently emitted in the broad line region and therefore is subject to scattering. Fig. 5 shows the spectrum in the region of CIV. There is an underlying broad component with $\text{FWHM} \sim 4000 \text{ km s}^{-1}$. Similar FWHM are often observed in high redshift quasars suggesting that it is scattered light.

The fit shows that the CIV line profile is not seriously affected by the underlying broad component due to the prominence of the "narrow" emission. This is usually the case (also for Ly α) and the studies that have found $\text{FWHM} \geq 1000 \text{ km s}^{-1}$ in the extended gas of HzRG are not affected by the effects of scattered light (McCarthy et al. 1996, Villar-Martín, Binette & Fosbury 1999). However, we cannot neglect this contribution when studying the line profiles in more detail (looking for different kinematic components, for instance); we would interpret the broad scattered components as due to extreme motions in the extended gas.

The best way to avoid any possible uncertainty on this issue is to compare with lines that are not emitted efficiently in the BLR (and, therefore, they are not scattered), such as HeII $\lambda 1640$ (Foltz et al. 1998, Heckman et al. 1991) or optical forbidden lines such as [OII] and [OIII] $\lambda 5007, 4959$ (the [OIII] lines might have a minor contribution from scattered light, di Serego Alighieri et al. 1997).

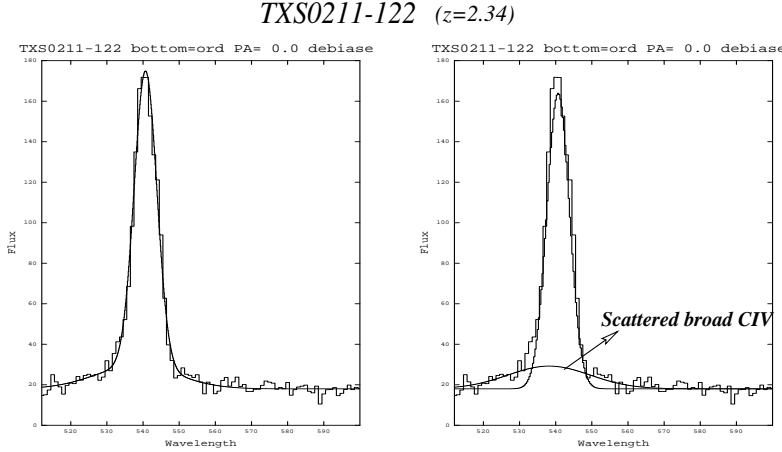


Fig. 5. TXS0211-122 is one the most highly polarized HzRG. Although broad scattered CIV seems to be present, it does not affect the narrow component, which dominates the emission. Right panel: fit and data. Left panel: individual components of the fit and data.

3.3. Resonant scattering of Ly α and CIV

Ly α and CIV $\lambda 1550$ are resonant lines and intervening HI and CIV respectively can absorb the emission. Ly α is particularly sensitive to this effect. The discovery of absorption troughs in the profile of the line across the whole extension of the Ly α emitting gas in many HzRGs has proved that Ly α absorption is a common phenomenon (van Ojik et al. 1997). CIV absorption troughs have also been observed (e.g. Binette et al. 2000). Van Ojik et al. found a correlation between the radio size and the occurrence of absorption, suggesting that in radio galaxies with large radio sources the effect is less worrying.

Absorption of Ly α photons can modify dramatically the profile of the line (van Ojik et al. 1997). Röttgering et al. (1997) concluded that the effects of associated H I absorption may be responsible for the shift of the Ly α line with respect to the high ionization lines in some objects. By using non resonant lines (HeII $\lambda 1640$, forbidden lines) we will avoid this problem. The CIV doublet, although resonant, is less sensitive and more reliable than Ly α . The use of high spectral resolution (~ 3 Å) can also help, since we will be able to resolve the absorption troughs (van Ojik et al. 1997).

3.4. The line doublets

The comparison between the FWHM of the emission lines provides information about the processes responsible for the line emission and the kinematics. The detection of different line velocity widths for different lines will lead us to the conclusion that different mechanisms are at work and/or there are regions of different physical conditions. As an example, some radio galaxies with radio/optical interactions show that low ionization lines are broader than high ionization lines (Clark et al. 1998). This has been interpreted

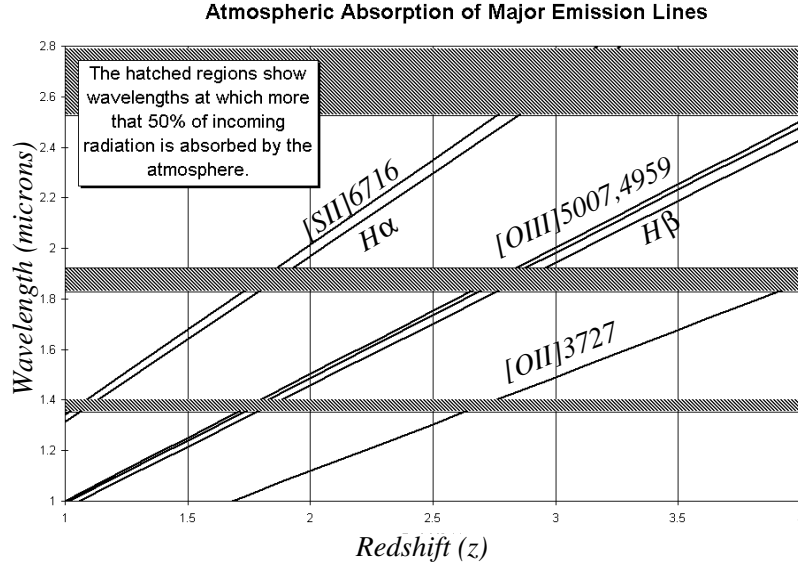


Fig. 6. The inclined solid lines indicate the variation with redshift of the observed wavelength for several important emission lines. The hatched regions show the spectral coverage of the atmospheric bands where the absorption is more than 50% of the incoming radiation. The redshifts for which one of the emission lines lies in these dark regions can be easily deduced from the plot.

as a consequence of shocks: the shocked gas has lower ionization level and more perturbed kinematics than the non perturbed gas.

In this sense, care must be taken with the doublets (CIV λ 1550, CIII] λ 1909 and [OII] λ 3727). At high redshifts the separation between the two components is large (7 \AA at $z = 2.5$ and 10 \AA at $z = 4$) and the doublet as a whole can show a profile apparently broader than single lines. This will be the case when the lines are similar in (observed) width or narrower than the doublet separation. If the lines are much broader the two components will be severely blended, whatever the resolution we use and the broadening will not be important. This should often be the case since gas motions can produce lines of intrinsic FWHM $\geq 20 \text{ \AA}$ at $z = 2.5$.

4. Optical vs. near infrared

The NIR spectral range offers some advantages compared to the optical. The lines (optical rest frame) are less affected by dust extinction. Moreover, we can use the same lines that have provided most of the information about low redshift objects. The comparison is therefore easier and more reliable than comparing the UV rest frame at high redshift with the optical rest frame at low redshift. We can also use the diagnostic tools developed for low redshift objects to investigate the physical conditions and ionization state of the

extended gas. Such diagnostic techniques are reasonably well understood, contrary to what happens in the UV rest frame.

The main problems we may find when observing in the NIR are due to the effects of the atmosphere and the thermal emission from the telescope. Due to atmospheric absorption some redshifts are forbidden to study certain emission lines (see Fig. 6).

On the other hand, HzRG are very faint sources and the OH bands (dominant source of sky emission in the NIR) are bright and variable compared to them so that in same cases it will be impossible to obtain enough S/N on the line of interest. Since the FWHM of the object lines is large (e.g. [OIII] $\lambda 5007 \sim 40-50 \text{ \AA}$ at $z=2.5$), the contamination will often be important independently of the spectral resolution we use, unless we work with emission lines that lie far from strong sky lines. This puts constrains on the object redshifts. At longer wavelengths ($\geq 2.2 \mu\text{m}$) the limitations are due to thermal background.

5. Summary and conclusions

We have discussed the possible uncertainties and proposed solutions for the interpretation of the kinematics of the extended gas in HzRG using the optical (UV rest frame) and NIR (optical rest frame) emission lines.

- The spectral decomposition of the emission lines will show multiple components. By studying the kinematic, flux and spatial properties of the individual components we can disentangle the mechanisms responsible for the extreme motions.
- The presence of several kinematic components (or absorption in the case of Ly α) may produce apparent rotation curves.
- Ly α absorption by neutral gas/dust can change dramatically the emission line profiles. CIV $\lambda 1550$ is also resonant, but less sensitive. The detection of non resonant lines with good S/N is important to understand the effects of resonant scattering.
- When scattered broad lines are present, they do not affect the emission line profiles of the brightest lines. However, they must be taken into account when studying different kinematic components, otherwise high velocity motions in the extended gas could be inferred. HeII $\lambda 1640$ and the forbidden optical lines can help to determine the contribution of scattered light.
- The doublets (CIV, CIII], [OII]) are noticeably broader than simple lines (like HeII) when the gas motions have dispersion velocities similar to the separation between the doublet components.
- NIR observations are better suited for kinematic studies of HzRG since they map optical rest frame lines that are less sensitive to dust and the effects mentioned above. An additional advantage is that this spectral range allows the comparison with studies

at low redshift so that we can use powerful diagnostics tools developed for nearby objects. However, the atmosphere sets limitations to this type of observations.

Acknowledgements. The authors thank the members of the ‘z2p5’ collaboration A. Cimatti, M. Cohen, B. Fosbury and B. Goodrich for the data presented in this paper for illustrative purposes. We thank Phil Lucas for useful discussions and Callum McCormick for providing Figure 6.

References

Baum S., McCarthy P., 2000, AJ 119, 2634

Binette L., Kurk J., Villar-Martín M., Röttgering H., 2000, A&A 356, 23

Chambers K.C., Miley G.K., van Breugel W., 1987, Nature 329, 604

Chambers K.C., 1998, in: American Astronomical Society Meeting, 193, 110.01

Cimatti A., Dey A., van Breugel W., Hurt T., Antonucci R., 1997, ApJ 476, 677

Cimatti A., di Serego Alighieri S., Vernet J., Cohen M., Fosbury R., 1998, ApJ 499, 21

Corbin M., Francis P., 1994, AJ 108, 2016

Clark N.E., Axon D., Tadhunter C.N., Robinson A., O’Brien P., 1998, ApJ 494, 546

di Serego Alighieri S., Cimatti A., Fosbury R., Hes R., 1997, A&A 328, 510

Foltz C., Chaffee F., Weymann T., Anderson S., 1988, in *QSO Absorption Lines: Probing the Universe*, ed. J.C. Blades, D. Turnshek & C. Norman (Cambridge: Cambridge University Press), p. 53

Fosbury R., Vernet J., Villar-Martín M., Cohen M., Cimatti A., di Serego Alighieri S., McCarthy P., 1999, in *ESO Conference on Chemical Evolution from Zero to High Redshift*, Garching, Germany, October 14-16 1998. ESO Astrophysics Symposia, Eds. J. Walsh and M. Rosa, Springer

Heckman T., Lehnert M., Miley G., van Breugel W., 1991, ApJ 381, 373

Hernquist L., 1993, ApJ 409, 548

Jackson N., Rawlings S., 1997, MNRAS 286, 241

Larkin J. et al., 2000, ApJL 533, 61

McCarthy P.J., Spinrad H., Djorgovsky S., Strauss M.A., van Breugel W., Liebert J., 1987, ApJ 319, L39

McCarthy P.J., Baum S., Spinrad H., 1996, ApJS 106, 281

McIntosh D., Rieke M., Rix H., Foltz C., Weymann J., 1999, ApJ 514, 40

Oke et al, 1995, PASP 107, 375

Röttgering H., van Ojik R., Miley G., Chambers K., van Breugel W., de Koff S., 1997, A&A 326, 505

Tadhunter C., Fosbury R., Quinn P., 1989, MNRAS 240, 225

Taniguchi Y., Shioya Y., 2000, ApJL 532, 13

van Ojik R., Röttgering H., Carilli C., Miley G., Bremer M., Macchetto F., 1996, A&A 313, 25

van Ojik R., Röttgering H., Miley G., Hunstead R., 1997, A&A 318, 358

Villar-Martín M., Binette L., Fosbury R., 1996, A&A 312, 751

Villar-Martín M., Binette L., Fosbury R., 1999, A&A 346, 7

Villar-Martín M., Tadhunter C., Morganti R., Axon D., Koekemoer A., 1999, MNRAS 307, 24